Raman scattering studies on multiferroic $YMnO_3$

2007 J. Phys.: Condens. Matter 19 365239

(http://iopscience.iop.org/0953-8984/19/36/365239)

IOP PUBLISHING JOURNAL OF PHYSICS: CONDENSED MATTER

J. Phys.: Condens. Matter **19** (2007) 365239 (9pp) doi:10.1088/0953-8984/19/36/365239

Raman scattering studies on multiferroic $YMnO_3$

H Fukumura[1], S Matsui[1], H Harima[1], K Kisoda[2], T Takahashi[3], T Yoshimura[3] and N Fujimura[3]

[1] Department of Electronics and Information Science, Kyoto Institute of Technology, Kyoto 606-8585, Japan
[2] Department of Physics, Wakayama University, Sakaedani, Wakayama 640-8510, Japan
[3] Department of Physics and Electronics, Osaka Prefecture University, Osaka 599-8531, Japan

E-mail: dj000091@djedu.kit.ac.jp

Received 21 December 2006, in final form 7 February 2007
Published 24 August 2007
Online at stacks.iop.org/JPhysCM/19/365239

Abstract

$YMnO_3$ is a multiferroic material in which ferroelectric and antiferromagnetic ordering can coexist. We have studied a $YMnO_3$ bulk crystal in detail by Raman scattering in a wide temperature range of 15–1200 K, with comparison to a previous experiment at room temperature and a theoretical prediction for Raman-active phonon modes. In the low-temperature ferroelectric phase, the observed phonon spectra showed anomalous temperature variation at the Néel temperature, $T_N \sim 80$ K, suggesting a coupling between the spin and phonon systems below T_N. Furthermore, spectra for the high-temperature paraelectric phase, reported here for the first time, showed a sudden change at the Curie temperature $T_C > 900$ K, suggesting an abrupt structural phase change from the ferroelectric to the paraelectric phase.

1. Introduction

Multiferroic materials showing ferromagnetism and ferroelectricity simultaneously are attracting much attention in the field of spin-electronics, because the coupling effect between the magnetic and ferroelectric orderings, the so-called magnetoelectric effect, may lead us to the development of future innovative devices [1, 2]. Unfortunately, however, only a limited number of materials have been identified as multiferroics, even if antiferromagnetic ordered systems are included in the category [3].

$YMnO_3$ in the hexagonal phase is one of the few multiferroic materials [4, 5] in which ferroelectric and anti-ferromagnetic ordering coexist. It has a Curie temperature of $T_C > 900$ K and a Néel temperature of $T_N \sim 80$ K [1, 6]. Using the ferroelectric properties, $YMnO_3$ was recently shown to be a candidate for nonvolatile memory [7]. Furthermore, anomalies in the dielectric constant were observed near T_N, indicating a coupling between the ferroelectric and the magnetic orderings [8].

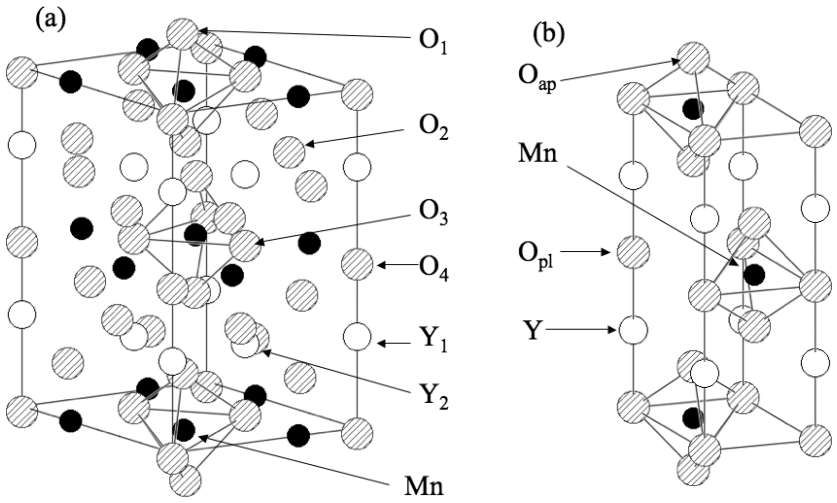

Figure 1. Crystal structure of $YMnO_3$ in its ferroelectric (a) and paraelectric (b) phases.

Raman spectroscopy is a powerful tool for studying lattice dynamics of solids and, if applied to multiferroics, it may bring us much information suitable for investigating the coupling mechanism between the ferroelectric and ferromagnetic (or antiferromagnetic) orderings. Recently, hexagonal $YMnO_3$ has been studied intensively by Iliev *et al* using Raman scattering and IR absorption [9]. They found many phonon signals and presented a detailed mode analysis. However, since their experiment was done only at room temperature, further studies covering the above critical temperatures are eagerly awaited. From this viewpoint, we observe here Raman spectra of $YMnO_3$ bulk polycrystal at 15–1200 K with phonon-mode assignment. Temperature variation of the phonon spectra showed clear evidence of spin-phonon coupling below $T_N \sim 80$ K. Abrupt spectral changes combined with a structural phase transition at $T_C > 900$ K are also reported.

2. Experimental details

2.1. Sample

Figure 1 shows the crystal structures of hexagonal $YMnO_3$, part (a) showing the low-temperature ferroelectric phase and part (b) the high-temperature paraelectric phase. The ferroelectric phase structure, which is a noncentrosymmetric system, belongs to the space group $P6_3cm$ (C_{6v}^3). The unit cell contains layers of corner-sharing MnO_5 bipyramids with a triangular base with nonequivalent O_3 and O_4 atoms, whereas the O_1 and O_2 occupy the apical sites. The Mn–O_1 and Mn–O_2 bonds are slightly tilted against the c-axis. The Y_1 and Y_2 atoms are located between the bipyramidal layers. On the other hand, the paraelectric phase structure, which is a centrosymmetric system, belongs to the space group $P6_3/mmc$ (D_{6h}^4). Here, the Mn–O_1 and Mn–O_2 bonds are parallel to the c-axis, and the triangular base of MnO_5 bipyramids is vertical to the c-axis. This means that the ferroelectric phase structure $P6_3cm$ is easily obtained from the simpler one, $P6_3/mmc$, by a small rotation of the MnO_5 bipyramids around an axis penetrating the Mn ion and parallel to one of the sides of the base triangle [10].

The elementary cell of the ferroelectric phase contains six formula units, while the paraelectric phase contains only two formula units and has a higher structural symmetry as seen

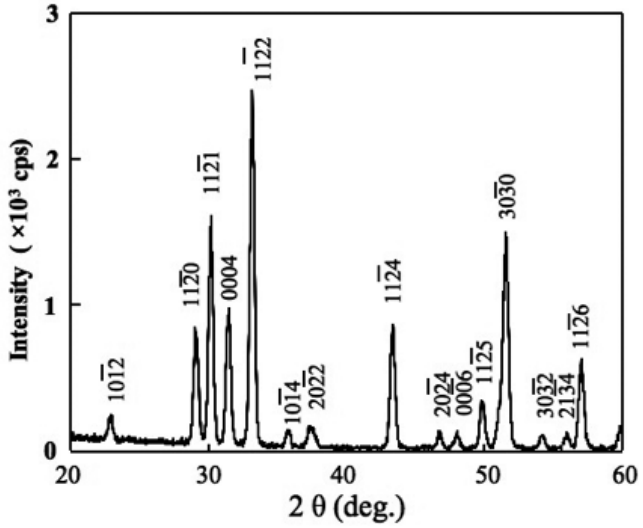

Figure 2. XRD pattern of a $YMnO_3$ sample.

in figure 1. Therefore, many fewer Raman-active phonon modes are expected in the paraelectric phase than in the other phase: there are 38 Raman-active phonon modes ($9A_1 + 14E_1 + 15E_2$) in the ferroelectric phase with possible TO–LO splitting for the A_1 and E_1 modes because of induced dipole moment. On the contrary, only five phonon modes ($A_{1g} + E_{1g} + 3E_{2g}$) are allowed in the paraelectric phase [9].

For this work we prepared sintered ceramic samples of stoichiometric composition. Figure 2 shows a typical x-ray diffraction (XRD) pattern of the samples at room temperature (ferroelectric phase). It shows only sharp peaks of $YMnO_3$, indicating that the samples have high crystalline quality and no secondary phases are included.

2.2. Raman measurement

For low-temperature measurements at 15–300 K, the samples were fixed to a cold finger in a closed-cycle He gas cryostat. Raman scattering was observed by using an Ar gas laser at 514.5 nm for excitation. The laser was focused by a lens at the sample surface, and the scattered light was collected in a quasi-back-scattering geometry to a double monochromator of focal length 85 cm. For high-temperature measurements at 300–1200 K, the samples were placed in an electrical furnace (Linkam LK-1500) put on a Raman microscope stage, and the back-scattered light was observed by the double monochromator. The spectra were observed by a liquid-nitrogen-cooled charge-coupled-device (CCD) detector.

3. Results and discussion

3.1. Low-temperature region

Figure 3 shows Raman spectra of $YMnO_3$ observed at 15–300 K in the ferroelectric phase. With the decrease of temperature from bottom to top, all the peaks become sharp and shift to a higher frequency. A total of 20 phonon peaks were clearly observed at low temperature, and classified to A_1, E_1 and E_2 modes by polarized Raman study and with reference to the previous results of

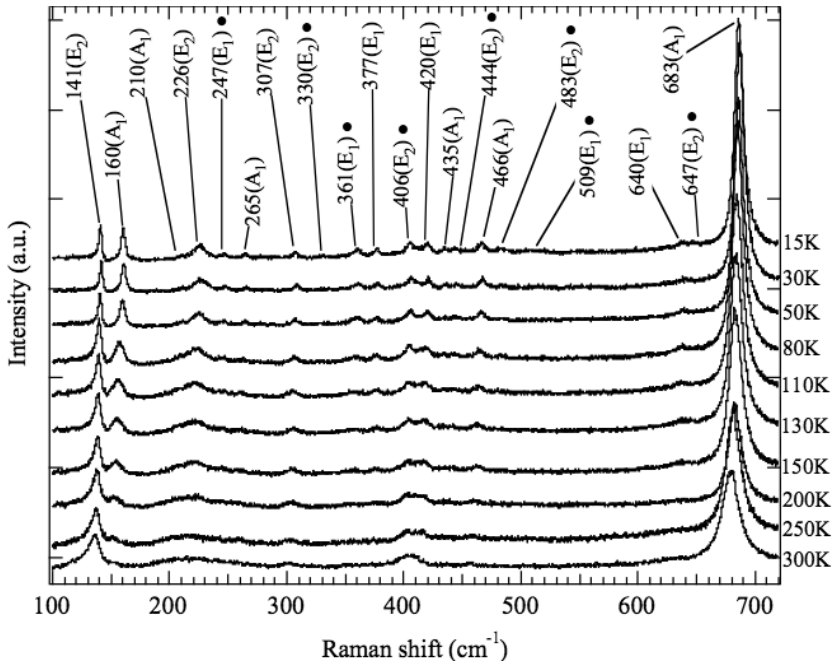

Figure 3. Raman spectra of $YMnO_3$ at 15–300 K. The phonon modes newly observed in this study are marked by filled circles.

Table 1. Observed phonon frequency of $YMnO_3$ (A_1 mode) with comparison to a previous study [9]. Values in parenthesis denote IR data.

	Obs. (cm^{-1})		Calc. (cm^{-1}) [9]
Mode	Ours (15 K)	Iliev [9] (300 K)	TO, LO
A_1	160	148	147, 147
A_1	210	190	204, 216
A_1	264	257 (265)	222, 269
A_1		297	299, 301
A_1		(398)	388, 398
A_1	435	433 (428)	423, 467
A_1	466	459	492, 496
A_1		(612)	588, 601
A_1	686	681	662, 662

Iliev *et al* [9]. Here, as suggested by Iliev *et al*, we neglect TO–LO splittings in our analysis. Eight phonon modes were newly observed in this study, as shown by filled marks in figure 3 with frequency in cm^{-1} and mode assignment. The results of our analysis are summarized in tables 1–3 for the A_1, E_1 and E_2 modes, respectively. There is a good agreement between our data and those of Iliev *et al* [9]. Many phonon modes, however, remain undiscovered, especially in the E_1 and E_2 mode. The listing of the phonon frequencies remains to be completed.

In figure 3 we find by careful inspection that some phonon modes show peculiar temperature variation: for example, the A_1 mode at 160 cm^{-1} suddenly shows a large frequency shift and peak broadening at around 80 K. The phonon frequency is plotted against the

Table 2. Same as table 1, but for the E_1 mode.

	Obs. (cm^{-1})		
Mode	Ours (15 K)	Iliev [9] (300 K)	Calc. (cm^{-1}) [9] TO, LO
E_1			117, 118
E_1			147, 149
E_1			158, 158
E_1		(211)	212, 231
E_1	247	(238)	233, 245
E_1		(281)	250, 337
E_1	360	(308)	353, 367
E_1	377	376	390, 403
E_1	420	408	410, 415
E_1		(457)	459, 477
E_1	509	(491)	492, 527
E_1			559, 559
E_1		(596)	586, 589
E_1	638	632	635, 635

Table 3. Same as table 1, but for the E_2 mode.

	Obs. (cm^{-1})		
Mode	Ours (15 K)	Iliev [9] (300 K)	Calc. (cm^{-1}) [9] TO, LO
E_2			71
E_2			108
E_2	141	135	136
E_2			161
E_2	225	∼215	212
E_2			241
E_2	307		245
E_2	331	302	336
E_2	406		382
E_2	444		407
E_2	483		458
E_2			515
E_2			557
E_2			580
E_2	647		638

temperature in figure 4 with some other modes showing similar behaviour. Here we tried to fit the phonon frequency variation by using a conventional formula assuming anharmonic phonon coupling processes for up to three phonons [11]:

$$\omega(T) = \omega_0 + A\left[1 + \frac{2}{e^x - 1}\right] + B\left[1 + \frac{3}{e^y - 1} + \frac{3}{(e^y - 1)^2}\right]. \quad (1)$$

Here, $\omega(T)$ is the phonon frequency at T (kelvin), $x = \hbar\omega_0/2kT$, $y = \hbar\omega_0/3kT$ with thermal energy kT, and A, B and ω_0 are the adjustable parameters. The dashed curves in figure 4 show the best fits to the observed results. As we can easily find in figure 4, the observed data show anomalous variation at around 80 K and cannot be fitted well by a single curve of equation (1). We can fit the data by using two best-fit curves as shown by the dashed curves. The phonon

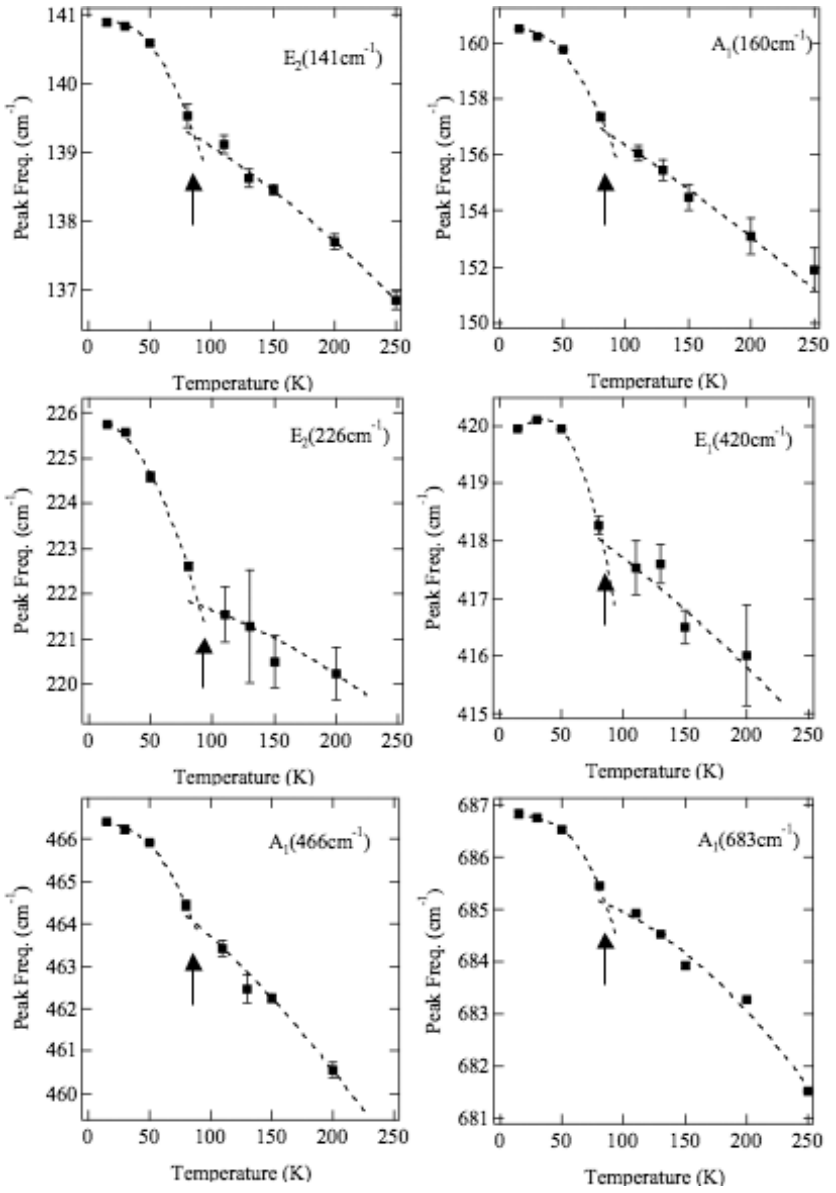

Figure 4. Frequency variation of phonon modes showing anomalous temperature dependence. Dashed curves show theoretical fits to the experimental data by considering anharmonic coupling effects for up to three phonons. An anomalous change appears at ∼80 K (arrow).

modes plotted here commonly suggest anomalous behaviour at ∼80 K. Recalling that the Néel temperature of $YMnO_3$ is $T_N \sim 80$ K, this anomalous variation suggests spin-phonon coupling that occurs in the magnetically ordered phase below T_N.

These anomalies are not induced by pure structural phase transformation because the phonon spectra in figure 3 show no apparent or drastic variation due to structural phase transition at $T_N \sim 80$ K. Similar anomalies observed in $SrRuO_3$ (ferromagnet) have been explained by ion motions that modulate the spin exchange coupling [12]. In $YMnO_3$, the

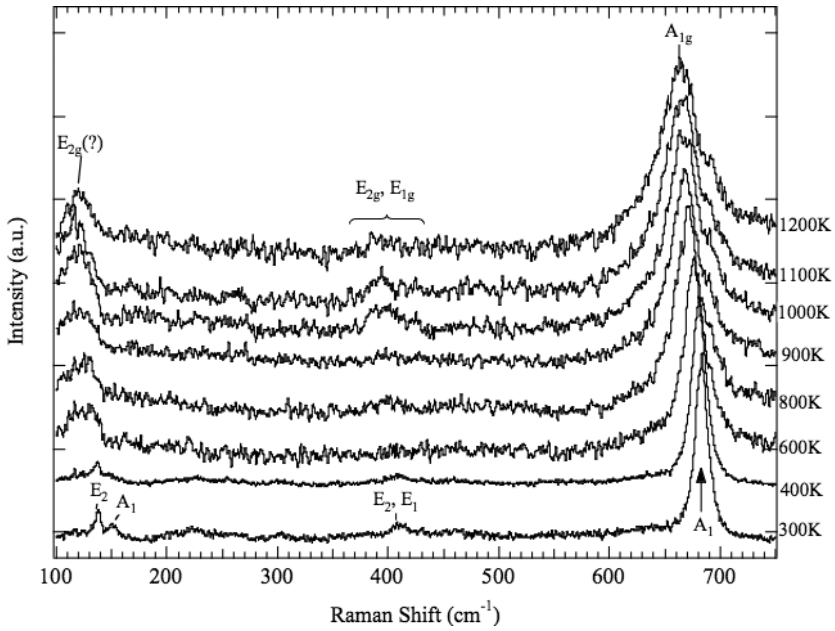

Figure 5. Raman spectra of $YMnO_3$ at 300–1200 K. The assignment of the E_{2g} mode at $\sim$120 cm^{-1} in the paraelectric phase is tentative.

E_2 mode (226 cm^{-1}) includes displacement of Mn, O_1, O_2 and O_3 ions in the *c*-plane (see figure 1) [9]. Therefore, the mode may effectively modulate the Mn–O–Mn bond angle in the *c*-plane and clearly present anomalous behaviour as seen in figure 4. On the other hand, other modes such as the A_1 mode (160 cm^{-1}), which includes displacement of Y_1 and Y_2 ions along the *c*-axis, also show the anomaly at $T_N \sim 80$ K. This is an indication of more complex spin-phonon coupling or a strong mixing of phonon modes [12].

3.2. High-temperature region

Figure 5 shows the temperature variation of Raman spectra for $YMnO_3$ at 300–1200 K. With increasing temperature from bottom to top, all the peaks become broader and shift to a lower frequency as we have seen in the lower-temperature region (figure 3). Between 900 and 1000 K, notable changes suddenly occur on the spectra: (a) new peaks appear at around 400 cm^{-1} and (b) the rate of frequency shift of the strong A_1 mode at 680 cm^{-1} (at 300 K) clearly changes, as seen in figure 6. By lowering the temperature from 1200 back to 300 K we confirmed that the spectra were reproduced at each temperature (not shown here). This means that the sample did not deteriorate during the heating process.

Recalling that the Curie temperature of $YMnO_3$ is $T_C > 900$ K, we believe that this anomaly corresponds to the structural phase change from the ferroelectric phase $P6_3cm$ to the paraelectric one $P6_3/mmc$. This transformation from the noncentrosymmetric structure ($P6_3cm$) to the centrosymmetric one ($P6_3/mmc$) is accompanied by a reduction of the unit cell volume as shown in figure 1. So, if this transformation is caused by only a small lattice distortion, each Γ-point phonon mode of the ferroelectric phase, which is Raman-active, has a zone-boundary counterpart mode in the paraelectric phase, which is Raman-inactive. Therefore, the number of Raman-active modes is much reduced in the paraelectric phase (5) from that in the other phase (38).

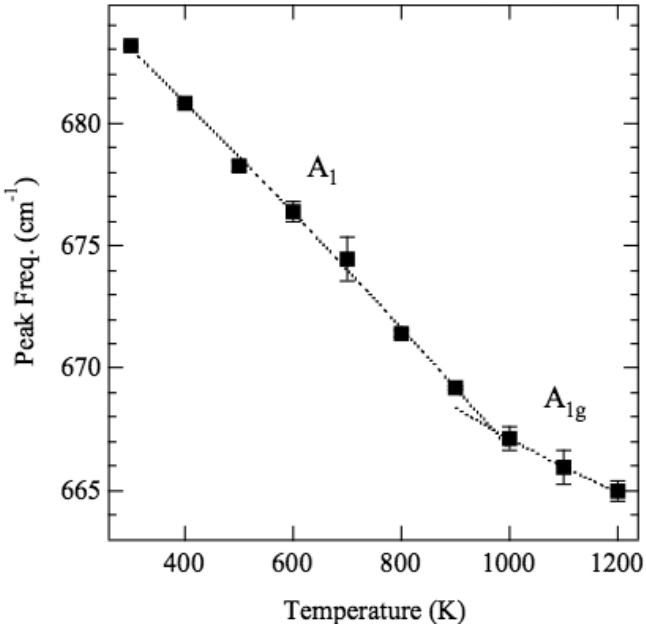

Figure 6. Frequency variation of the A_1 and A_{1g} modes. Dashed curves show theoretical fits to the experimental data by considering anharmonic coupling effects for up to three phonons.

Table 4. Observed phonon frequency of $YMnO_3$ in the paraelectric phase with comparison to a previous study [9].

Ode	Obs. (cm^{-1}) (1100 K)	Calc. (cm^{-1}) [9]
A_{1g}	664	666
E_{1g}	∼420	402
E_{2g}	∼120 (?)	107
E_{2g}	∼395	395
E_{2g}		498

From this consideration, the strong A_1 mode at 680 cm^{-1} (at 300 K) in the ferroelectric phase transforms to the A_{1g} mode in the paraelectric phase, and the weak E_1 and E_2 modes at ∼400 cm^{-1} transform to the E_{1g} and E_{2g} modes likewise, as shown in figure 5. On the other hand, the ferroelectric phase shows E_2 and the A_1 modes at about 137 and 150 cm^{-1}, respectively, at 300 K. These modes correspond to the displacement of Y_1 and Y_2 ions in the *c*-plane and along the *c*-axis, respectively. They disappear in the paraelectric phase since they transform to zone-boundary modes. As listed in table 4, the observed phonon frequencies at 1100 K show very good agreement with theoretical predictions for the paraelectric phase [9]. Our observation suggests that the phase change accompanied by tilting of MnO_5 polyhedrons (see figure 1) occurs suddenly at T_C.

4. Conclusion

We investigated a multiferroic material, $YMnO_3$, by Raman scattering in the temperature range of 15–1200 K for both the low-temperature ferroelectric phase and the high-temperature paraelectric phase. In the ferroelectric phase we observed 20 phonon modes. The phonon

frequencies were compared with previous room temperature data and a theoretical mode prediction, and eight phonon modes were newly observed in this study. Some phonon modes showed anomalous temperature variation at the Néel temperature, $T_N \sim 80$ K, suggesting a coupling between the spin and phonon systems below T_N. Furthermore, the spectra for the high-temperature paraelectric phase showed a sudden change at the Curie temperature $T_C > 900$ K. This suggests an abrupt structural phase change accompanied by a small rotation of MnO_5 polyhedral units in $YMnO_3$.

References

[1] Smolenskii G A and Chupis I E 1982 *Sov. Phys.—Usp.* **25** 475
[2] Schmid H 1994 *Ferroelectrics* **62** 317
[3] Hill N A 2000 *J. Phys. Chem.* B **104** 6694
[4] Gilleo M A 1957 *Acta Crystallogr.* **10** 161
[5] Yakel H, Koehler W C, Bertaut E F and Forrat F 1963 *Acta Crystallogr.* **16** 957
[6] Lukaszewicz K and Karut-Kalicinska J 1974 *Ferroelectrics* **7** 81
[7] Fujimura N, Ishida T, Yoshimura T and Ito T 1996 *Appl. Phys. Lett.* **69** 1011
[8] Huang Z J, Cao Y, Sun Y Y, Xue Y Y and Chu C W 1997 *Phys. Rev.* B **56** 2623
[9] Iliev M N, Lee H-G, Popov V N, Abrashev M V, Hamed A, Meng R L and Chu C W 1997 *Phys. Rev.* B **56** 2488
[10] van Aken B B, Palstra T T M, Filippetti A and Spaldin N 2004 *Nat. Mater.* **3** 164
[11] Balkanski M, Wallis R F and Haro E 1983 *Phys. Rev.* B **28** 1928
[12] Iliev M N, Litvinchuk A P, Lee H-G, Chen C L, Dazneti M L, Chu C W, Ivanov V G, Abrashev M V and Popov V N 1999 *Phys. Rev.* B **59** 364